This is the Pre-Published Version.
Q. Xie, Z. Zhang, S. Lin, Y. Qu, X. Huang (2020) *Smoldering Fire of High-Density Cotton Bale Under Concurrent Wind*. **Fire Technology**. https://doi.org/10.1007/s10694-020-00975-1
This is a post-peer-review, pre-copyedit version of an article published in Fire Technology. The final authenticated version is available online at: https://doi.org/10.1007/s10694-020-00975-1.

Smoldering fire of high-density cotton bale under concurrent wind

Qiyuan Xie[1,*], Zhigang Zhang [1], Shaorun Lin[2*], Yi Qu[3], Xinyan Huang[2,*]

[1]*State Key Lab of Fire Science, University of Science and Technology of China, Hefei 230027, China*

[2]*Department of Building Services Engineering, Hong Kong Polytechnic University, Hong Kong, China*

[3]*Zhengzhou Cotton & Jute Engineering Technology and Design Research Institute, Zhengzhou, 450018, China*

Abstract:

Cotton is the most widely used natural textile fiber for human beings, and fire safety during transportation, storage, and manufacturing is of great significance. This work investigated the smoldering burning of a high-density cotton bale (36 L and 225 kg/m^3) tightened by thin steel wire ropes under the concurrent wind. Without wind, the creeping smoldering spread showed two stages: (I) the relatively fast surface spread until the smoldering front covered the entire free surface (13 cm/h), and then (II) the slow in-depth spread from the surface to the internal (4 cm/h). With a concurrent wind, only one major concurrent smoldering front was observed from the free surface to the internal fuel, where the rate of smoldering spread decreased as the depth increased. The smoldering spread rate and peak temperature were found to increase almost linearly with the wind velocity due to the enhanced oxygen supply. The steel wire rope could appreciably obstruct the free-surface spread and slow down the overall smoldering spread. A large wind occasionally led to a smoldering-to-flaming transition, but the flame could not be sustained. This research improves our understanding of the wind effect on the smoldering spread in the compressed porous biomass and helps evaluate the fire risk of cotton during transportation and storage.

Keywords: smoldering spread pattern; external wind; fire spread rate; smoldering temperature; smoldering-to-flaming transition

1. Introduction

Cotton is the most important and necessary natural textile fiber for manufacturing apparels, home furniture as well as industrial products all around the world [1]. In 2013, the world cotton production was about 25 million tones or 110 million standard bales (~ 140 cm × 80 cm × 50 cm), and its agriculture land accounted for 2.5 % of the world's arable land [2]. Along with the continual increase in cotton production over the past few decades, more large-scale outdoor storage areas and warehouses have been built worldwide for storing tons of cotton bales, as shown in Fig. 1(a). Because of its flammable nature and the large fuel load in the storage unit, the fire risk of cotton bales becomes a significant concern. For example, several recent catastrophic warehouse fire accidents in China [3, 4] were primarily caused by the spontaneous ignition and fire spread on cotton bales (Fig. 1b), leading to many casualties and tremendous economic losses. Thus, a scientific understanding of the smoldering dynamics of cotton bales is critical for both fire prevention and the development of new fire suppression technologies.

For inquiries, please contact Qiyuan Xie xqy@ustc.edu.cn and Xinyan Huang xy.huang@polyu.edu.hk

Fig. 1. (a) Tons of cotton bales stored in an outdoor storage area, and (b) fire accident in a cotton-bale warehouse in Xinjiang, China (https://china.huanqiu.com/gallery/9CaKrnQhmQC).

Many studies in the literature focused on the ignition characteristics of small cotton samples or cotton products [5–9], and the influences of external factors (e.g., the level of irradiation and ignition/heating sources) and fuel properties (e.g., chemical composition, density, and size). For example, Wakelyn and Hughs [9] evaluated the forced smoldering ignition risk of cotton bales by cigarettes, match, and flame, as well as, the potential for self-heating ignition. Gaan and Sun [10] studied the influence of additives on the thermo-oxidative decomposition and heat of the flaming combustion of cotton. Luo et al. [11] studied the self-ignition of cotton and defined the ignition limit by the thermal decomposition temperature of around 210 ºC. Hagen et al. [6] investigated the ignition of cotton by a hot plate and showed an increase in the density of cotton led to a decrease in ignition temperature. Interestingly, they found that cotton samples exposed to a small heat flux (1.43 kW/m^2) would be ignited at a temperature that is lower than those exposed to a large heat flux (12.8 kW/m^2) [5]. It may be because a small heat flux only facilitates the self-ignition process of the smoldering fire, rather than directly heats the sample to the char oxidation temperature [12].

Most biomasses will char after heating, so they can sustain both smoldering and flaming combustion [13], such as cotton [7, 8], wood [14, 15] and peat soils [16]. For cotton, the transition between flaming and smoldering combustion has been observed [7, 17]. Unlike flaming, smoldering is the slow, low-temperature, and flameless burning of porous fuel, and it is the most persistent type of combustion phenomenon [18]. Hagen et al. [7, 8] suggested that the smoldering of cotton could produce gaseous fuel, and the secondary char oxidation might be the mechanism for the transition from smoldering to flaming combustion. However, in their experiments, the flames can only sustain for several minutes, different from those in pine needles [19] and PU foam [20] where flame could sustain to burnout the fuel.

Two mechanisms control the spread of smoldering combustion: oxygen supply and heat losses [18, 21]. The effect of wind on the smoldering ignition and fire spread has been studied for wood [22], pine needles [19], peat [23], and polyurethane foam [24–27]. Smoldering is a three-dimensional volumetric phenomenon, and the motion of smoldering has two modes, that is, (I) surface smoldering spread over the interface between fuel and ambient, and (II) internal smoldering spread inside the porous fuel [12]. For most internal smoldering spread, the oxygen supply usually controls the smoldering spread [28–30]. Rates of smoldering fire spread and burning will first increase with the airflow velocity (either the concurrent or opposed wind) unless near the blowoff [28]. Wang et al. [31] explored the burning of small cotton samples (26 cm × 10.5 cm × 10 cm) with a density of 150 kg/m^3 (uncompressed) under the concurrent wind. They observed smoldering spread was faster on the surface than the internal but did not quantify the spread rate, and the glowing phenomenon became intensive but not transitioned to a flame. Note that massive densely packed (compressed) cotton bales are often stored outdoor (Fig. 1a), posing a significant self-ignition and fire risk. Therefore, it is urgent to fully understand the smoldering

dynamics of cotton bales and then propose effective fire prevention technologies.

In this work, a small wind-tunnel with a burning chamber was designed to study the smoldering spread of cotton bales without wind and under a concurrent wind up to 2.8 m/s. The high-density compressed cotton bales stored in the warehouse were tested. Different fire phenomena and smoldering spread modes are discussed, and the smoldering spread rate, the peak temperature, and effects of wind and depth are quantified and analyzed in detail.

2. Experimental Method

All experiments were conducted in a small wind tunnel, and a burning chamber (100 cm × 60 cm ×60 cm) was designed in the center, as illustrated in Fig. 2. A fan was installed at the end of the wind-tunnel to induce airflow into the fire section, and the airflow was unified by the honeycombed panel with 1-mm mesh at the inlet and outlet section with a diameter of 10 cm. A digital anemometer (Smart Sensor AS 8336) was used to calibrate the wind velocity with an uncertainty of 3%. The top of the wind tunnel was made of a transparent glass panel, above which a CCD (charge-coupled device) video camera was installed to monitor the top-view burning process.

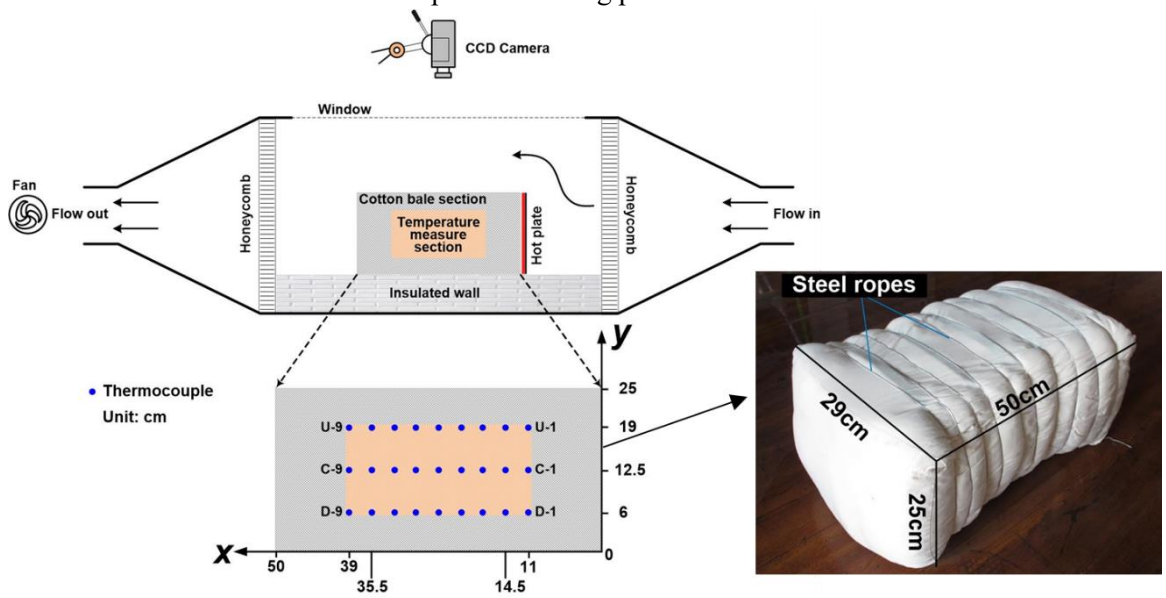

Fig. 2. Schematic of the experimental setup and the photo of the densely packed cotton bale.

The cotton in this study was harvested and processed in Xinjiang, China. The densely packed (compressed) cotton bale was wrapped with a thin cotton bag and fixed with 10 rounds of 1.6-mm thin steel wire ropes into a hexahedral package. The cotton bale had a mass of 8,100 g (±5% relative uncertainty) and a rough dimension of 50 cm × 29 cm × 25 cm (or about 36 L), as shown in Fig. 2. The bulk density was calculated to be about 225 kg/m^3, which was much higher than those uncompressed samples in the literature (20-150 kg/m^3) [5–7, 31]. The cotton sample was naturally dried in a chamber with a constant humidity of 50% for 72 h, and then the moisture content was measured to be about 8%. The thermogravimetric analysis (TGA) and differential scanning calorimetry (DSC) analysis of this cotton were conducted under both nitrogen and air atmospheres (see Appendix).

A series of experiments were conducted to investigate the smoldering spread of cotton bales with the applied wind velocity of <0.01 m/s (no forced wind except for small ventilation), 0.9 m/s, 1.6 m/s, 2.1 m/s and 2.8 m/s, respectively. Before experiments, the cotton bale sample was carefully placed on the insulation wall inside the wind tunnel. To initiate stable smoldering combustion in the cotton bale, the right-hand edge of cotton bale was ignited by a plate heater (30 cm × 30 cm × 0.2 cm) at 350 ºC for 2 min for all cases. To monitor the temperature and location of the smoldering front, 27 K-type thermocouples with the same bead diameter of 2 mm (a 3 × 9 matrix) were inserted into the vertical

central plate of heights, namely, 19 cm (U), 12.5 cm (C) and 6 cm (D) in Fig. 2, with respect to -6 cm, -12.5 cm and -19 cm from the top free surface. In each horizontal row, 9 thermocouples had an interval of 3.5 cm, starting from x = 11 cm to 39 cm. The temperatures are monitored and captured with an interval of 1 s. All experiments were repeated at least twice to reduce random errors. During experiments, the ambient temperature is 20 ± 2 ℃, and the relative humidity is about 50 ± 10 %.

3. Results and Discussion

3.1. Surface smoldering spread

Figure 3 shows a group of top-view images for the free-surface smoldering spread processes (a) without concurrent wind, and (b) under a 2.8-m/s concurrent wind, where arrows show different directions of smoldering spread. The original video link could be found in Appendix (Video 1 and 2). As being closer to the ambient oxygen, the smoldering fire first spread over the free surface. Without wind, it took about 300 min for igniting the entire free surface (Fig. 3a), as indicated by the motion of charring front on the cotton surface (Stage I). Because the oxygen supply was very limited without a concurrent wind, the in-depth spread toward the internal cotton bale was negligible in this stage. Afterward, the smoldering front started to spread in-depth (Stage II), which was difficult to observe by the regular camera from the top view.

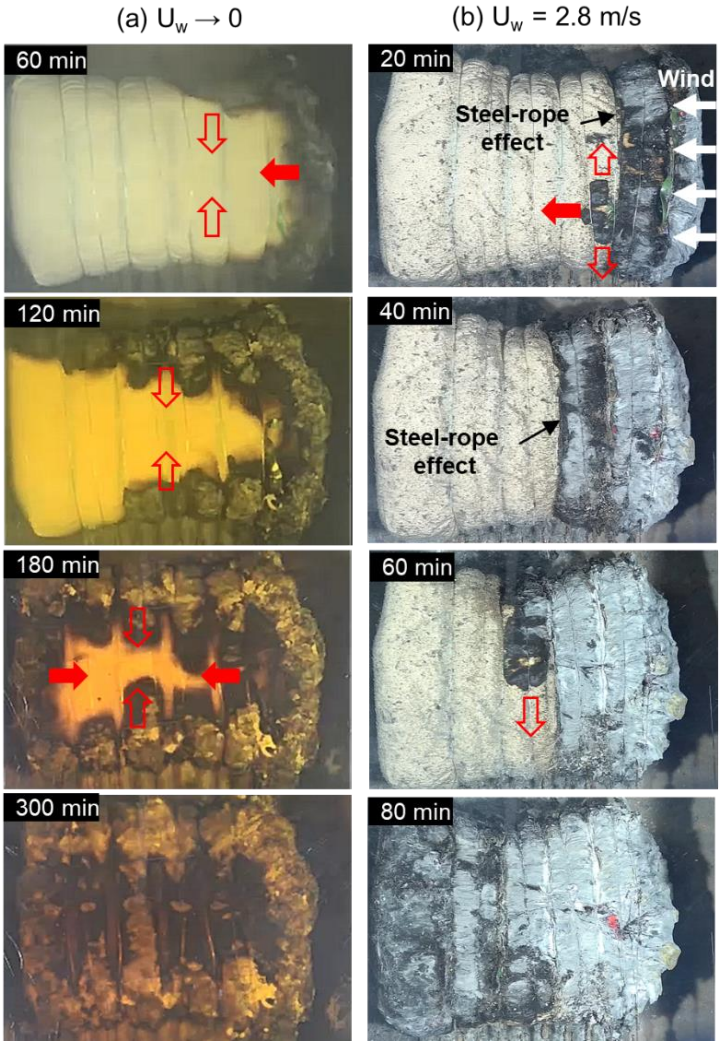

Fig. 3. The top-view images for smoldering fire spread over the cotton bale surface (a) without wind from Video 1, and (b) under the concurrent wind velocity of 2.8 m/s from Video 2, where the solid and hollow arrows represent the concurrent/opposed and traverse spread, respectively.

With the concurrent wind velocity of 2.8 m/s (Fig. 3b), the free-surface smoldering spread only lasted for less than 100 min. Along with the surface spread, the regression of cotton bale was also observed in the windward side due to the burnout of fuel, where some inserted thermocouples were exposed to the environment. Therefore, as the smoldering spread over the top surface, there was also a simultaneous concurrent smoldering spread inside the cotton bale (see more details in *Section 3.2*).

3.2. Effect of steel wire rope

Under the influence of steel wire rope, the finger-like smoldering spread pattern [34, 35] is observed, especially for the no-wind case (Fig. 3a). That is, as the free-surface smoldering front approached the steel wire ropes, it is restrained, but the smoldering front can still spread freely in the transverse directions. After a few minutes, the smoldering front crosses the steel wire rope and then spreads forward, until it is blocked by the next rope. Figure 4 further illustrates the influence of the steel wire rope on the local smoldering spread process.

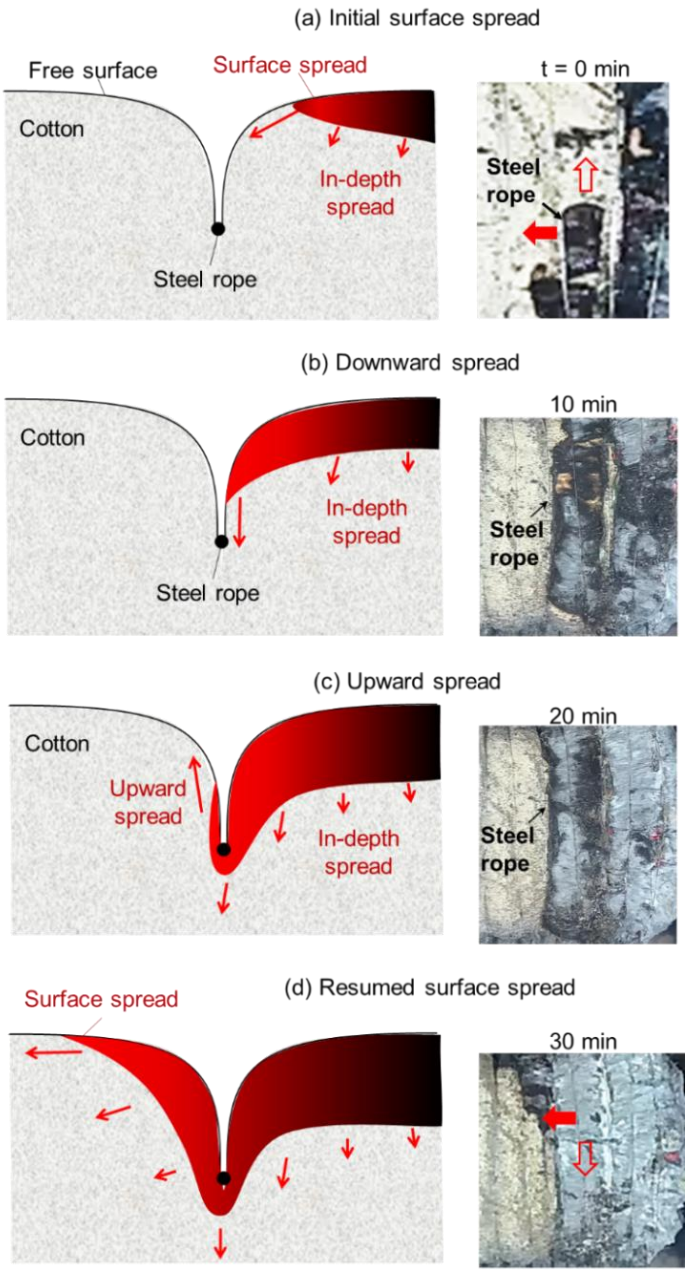

Fig. 4. Schematic diagrams and photos for smoldering spreading cross the steel wire rope, (a) initial surface spread, (b) downward spread, (c) upward spread, and (d) resumed surface spread.

Initially, the smoldering front quickly spread over the free surface while slowly spreading in-depth (Fig. 4a). As the smoldering front gradually approached to the imbedded rope (Fig. 4b), the smoldering spread slowed down and became restrained, because (1) the oxygen supply into the gap became limited, (2) the local density of cotton was increased, as it was strongly compressed by the steel wire rope, and (3) the large conductive heat loss through steel wire ropes.

In order to cross this local barrier, the smoldering front had to first spread in-depth below the steel wire rope and then spread upward again to reach the free surface (Fig. 4c). Such a by-pass process was very slow, which could last for 10 - 20 min, and it was not uniform along the steel wire rope, so that some smoldering hot spots could be first observed on the other side of the rope. At the same time, the free-surface smoldering front continued to spread in transverse directions, which showed the finger-like pattern. In some cases, even if the smoldering front ignited the entire block surface behind, it still took another several minutes to cross the steel wire rope. Therefore, the overall concurrent smoldering spread rate was remarkably reduced due to the existence of steel wire ropes.

3.3. Internal smoldering spread

Inside the porous fuel, the smoldering spread process is usually oxygen-limited [12, 18]. According to the temperature measurement of the thermocouple matrix, the internal temperature contour of the central plane can be mapped to help analyze the internal (or in-depth) smoldering spread process inside the cotton bale. Figure 5 shows the processed thermal images for the smoldering spread over cotton bale without wind (< 0.01 m/s), with respect to Fig. 3(a) and Video 1. The video of mapped thermal images could be found in Video 3 of the Appendix. The thermogravimetric analysis (TGA) in the Appendix indicates the decomposition of this cotton occurs at about 250 ℃, so that the trace of 250 ℃ contour roughly indicates the leading edge of the smoldering front. Initially, the smoldering front mainly existed and spread on the free surface (Stage I), because of the limited oxygen supply. After 300 min, the free-surface smoldering spread completed, and the cotton bale was covered by a hemispherical smoldering front, as indicated in Fig. 5(a).

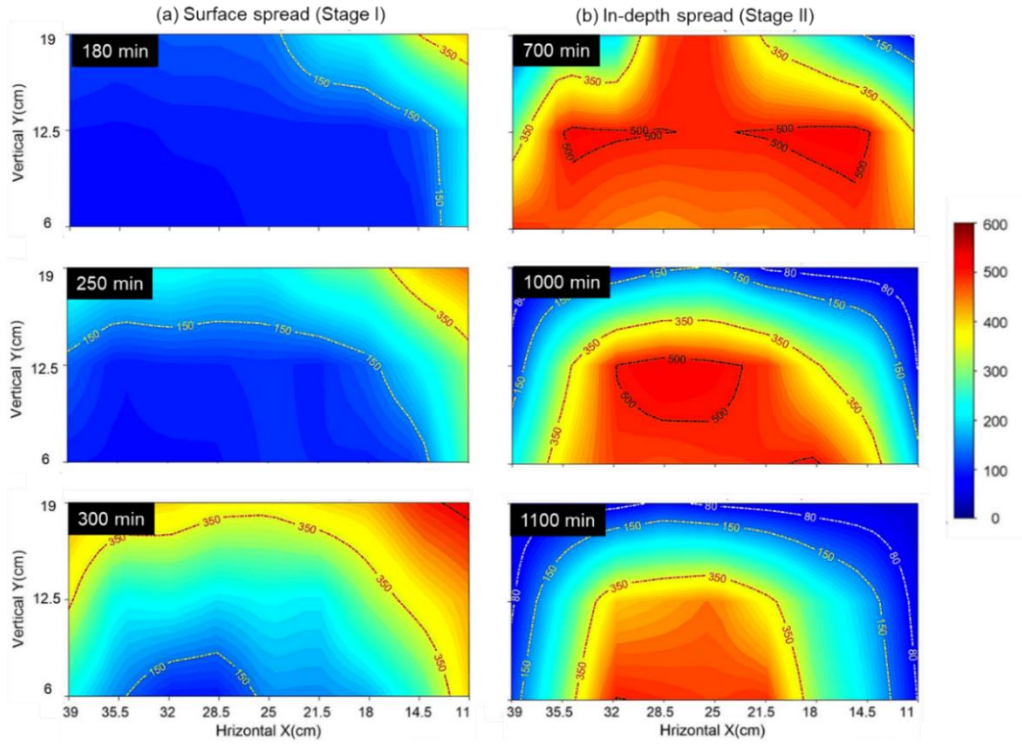

Fig. 5. Smoldering spread in the cotton bale with the wind velocity of 0.01 m/s (front video) based on the experimental measurement of thermocouple matrix, where the trace of 250 ℃ contour roughly indicates the leading edge of the smoldering front (a) Stage-I surface spread, and (b) Stage II in-depth spread (Video 2).

Afterward, the smoldering fire started to spread in-depth from the surface to the internal along with the shortest path of the oxygen flow (Stage II), as shown in Fig. 5(b). Without wind (or very small wind velocity), the oxygen could only enter the densely packed cotton bale by diffusion, where the consumption of oxygen created a low oxygen concentration (lean) at the smoldering front. The rate of in-depth spread radially towards the bottom center was uniform in all directions, and the peak smoldering temperature continued to increase because the accumulation of ash layer reduced the environmental heat loss. The Stage-II in-depth spread was much slower, which lasted for another 15 h. Eventually, the whole cotton bale sample was burnt out into ash after about 24 h. As the burning continued, the steel wire ropes lose the tension on the charred cotton which first expanded freely and then shrank due to further oxidation. The final residue was a mixture of white ash and unburnt black char, which has a grey color and mass of 180 ± 5 g. In other words, the residue mass was only 2% of the original mass.

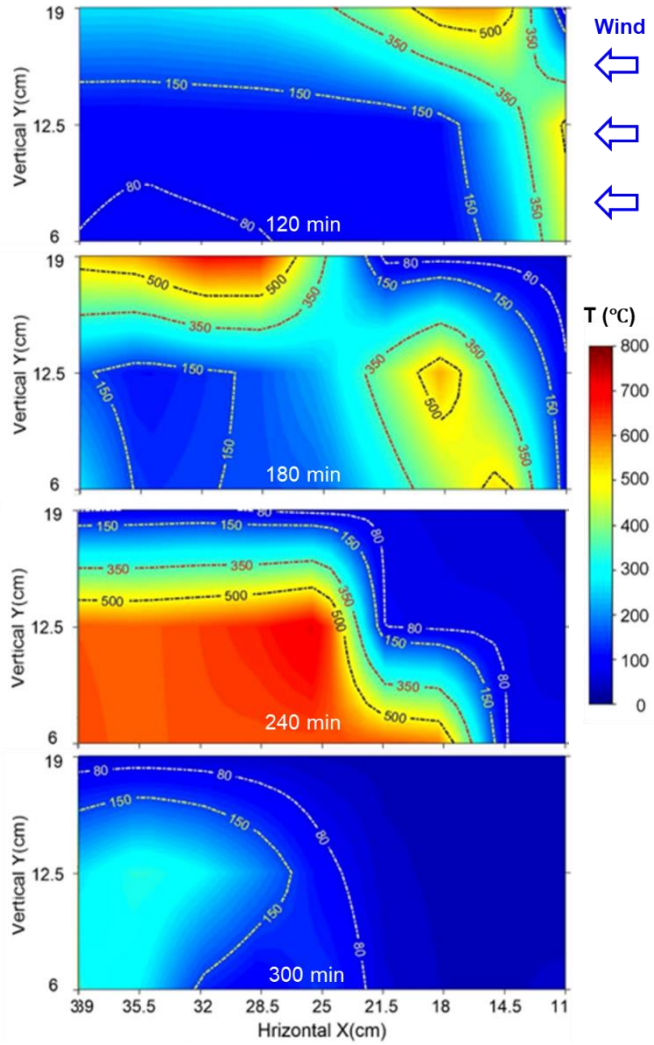

Fig. 6. Smoldering spread in the cotton bale with the wind velocity of 2.82 m/s (front video) based on the experimental measurement of thermocouple matrix, where the original video link can be found in (Video 4).

Figure 6 shows the thermal image for the internal smoldering spread over cotton bale under the concurrent wind velocity of 2.8 m/s, with respect to Fig. 3(b) and Video 2. The video of mapped thermal images could be found in Video 4 of the Appendix. Compared to the smoldering spread without the wind in Fig. 5, there is a big difference in terms of the internal smoldering spread pattern, reflecting the significant influence of the concurrent wind. With wind, only one primary internal spread front was

observed, which spread in the same direction as the concurrent wind. The spread rate closer to the free surface was much faster than the internal spread, because of the larger oxygen supply.

Moreover, under a large wind speed, a clear glowing phenomenon was observed on the free surface, where the local smoldering front was hot enough to emit visible light [12]. Sometimes, the smoldering-to-flaming (StF) transition could occur (see more details in Section 3.6). Because of the recirculation in the wake region on the left corner, the backward smoldering sub-front was also formed near burnout. Compared to the no-wind case, the smoldering spread was much faster under the wind, and the entire sample burnt out within 6 h. The residue mass was also only 2% of the original mass.

3.4. Smoldering spread rate

Figure 7(a) quantifies the effect of the concurrent wind velocity (U_w) on the free-surface smoldering spread rate without the steel-rope effect (V_{sur}) and the overall concurrent smoldering spread rate (V_{con}) that is influenced by the steel wire rope. As the wind velocity increases, both rates of the surface spread and the overall concurrent spread increased dramatically. For example, as the wind velocity increases from 0.9 m/s to 2.8 m/s, the free-surface spread rate increases from 42 cm/h to 66 cm/h. This trend also agrees with the concurrent flame spread [37] and smoldering spread [23, 28, 38] of other combustibles.

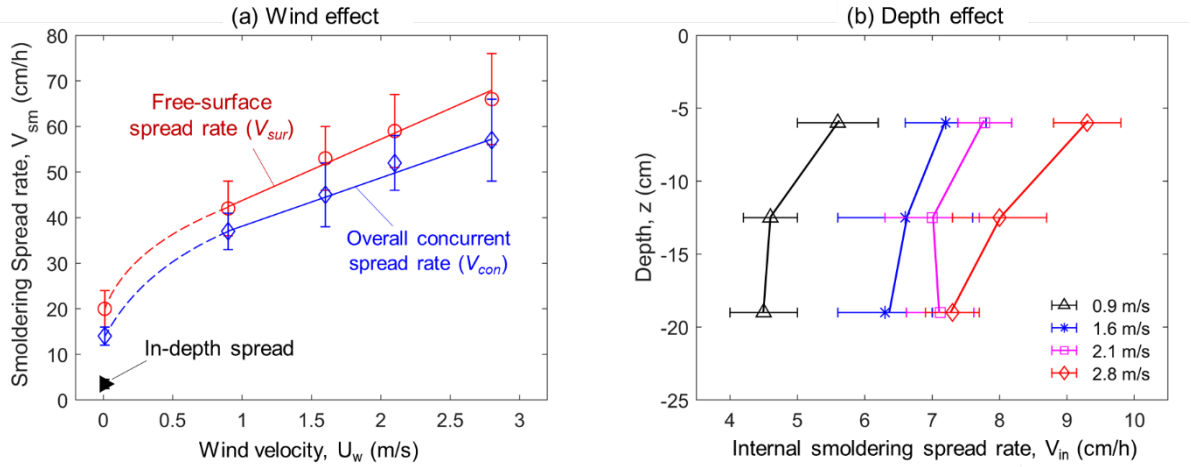

Fig. 7. (a) Rates of free-surface smoldering spread (V_{sur}) and overall concurrent smoldering spread (V_{con}) vs. concurrent wind speed (U_w), and (b) spread-rate profiles of internal concurrent smoldering (V_{in}) inside the cotton bale under different wind velocities. The symbols represent the average values and error bars indicate the standard deviations.

Specifically, under the concurrent wind, $U_w > 0$ [m/s], the smoldering spread rate [cm/h] can be fitted linearly with the wind speed as

$$V_{sur} = 13U_w + 31 \quad (1)$$

$$V_{con} = 11U_w + 28 \quad (2)$$

where R^2 coefficients for both linear fits are 0.98. Also, the existence of steel wire rope reduces the overall concurrent smoldering spread rate by about 5~10 cm/h, and the difference slightly increases with the wind speed. Without wind, the surface spread is much slower, because the oxygen supply is controlled by diffusion rather than convection. In addition, the rate of in-depth smoldering spread (4 cm/h) is remarkably lower than the surface spread, because it is more difficult for oxygen to diffuse into the porous cotton bale. Note that these empirical correlations are sensitive to the experimental setup and environmental conditions.

Figure 7(b) shows spread-rate profiles of internal concurrent smoldering inside the cotton bale

under different wind velocities. Compared to Fig. 7(a), the spread rate of internal smoldering (V_{in}) is almost one order of magnitude smaller than that of the free-surface smoldering, because of the limited oxygen supply. The internal smoldering spread rate also increases with the wind velocity like the free-surface smoldering spread. Nevertheless, the internal smoldering spread is less influenced by the external wind, because only limited air can enter the compressed cotton bale. Moreover, the internal smoldering spread rate increases as the depth below the top free surface is decreased, because of the additional oxygen supply from the top free surface. For example, under the wind velocity of 2.8 m/s, the internal spread rate decreases appreciably from 10 cm/h at 6-cm depth to 7 cm/h at 19-cm depth. A similar trend has also been observed in the smoldering spread over dry wood-based fibers [39] and organic soil [23].

A typical concurrent smoldering spread could be similar to a burning or fuel-regression process, like the burning of a candle or the premixed flame [12, 29]; thus, the concurrent smoldering spread rate may be calculated as regression rate ($\dot{R}$):

$$V_{in} = \dot{R} = \frac{\dot{m}_F''}{\rho_F} = \frac{\dot{m}_a''}{\gamma_a \rho_F} = \frac{\rho_a}{\gamma_a \rho_F} U_{w,in} \propto U_{w,in} \tag{3a}$$

where $\dot{m}_F''$ is the burning flux, ρ_F is the density of fuel, ρ_a is the density of air, $U_{w,in}$ is the air velocity inside the porous fuel, $\dot{m}_a'' = \rho_a U_a$ is the mass flux of air supply, and γ_a is the stoichiometric coefficient of air.

Based on the Darcy Law, $U = -(K/\mu)(dP/dx)$ and the Bernoulli Equation ($\Delta P = \rho U^2/2$), the airflow inside the porous media can be estimated as

$$U_{w,in} = -\frac{K}{\mu}\frac{\Delta P}{\Delta x} \propto \frac{U_w^2}{\Delta x} \tag{4}$$

where K is the permeability, μ is the gas viscosity, ΔP is the pressure gradient, and Δx is the characteristic distance inside the porous media. Thus, the internal concurrent smoldering spread rate should also have a similar form as $V_{in} \propto U_w^a/\Delta x^b$. Based on the experimental data in Fig. 7(b), an empirical correlation for V_{in} [in cm/h) as a function of external concurrent wind speed (U_w) [m/s] and the depth from top free surface (d) [cm] can be obtained

$$V_{in} = 6.4\frac{U_w^{0.5}}{d^{0.1}} \tag{3b}$$

where the R^2 coefficient for this nonlinear fit is 0.97. Compared to the linear increase of the surface smoldering spread in Eq. (1-2), the internal smoldering spread is relatively less sensitive to the external wind. Because the concurrent smoldering spread is also proportional to the burning rate of fuel (Eq. 3a), it also explains the experimental observation of the decreasing burning duration with the increasing wind velocity.

3.5. Peak smoldering temperature

Figure 8 compares the smoldering peak temperature under different wind velocities. Similar to the smoldering spread rate, the peak temperature also increases as the wind velocity increases [23, 40]. For example, as the wind velocity increases from near zero to 2.8 m/s, the smoldering peak temperature increases from 510 °C to 750 °C. Specifically, under the concurrent wind ($U_w > 0$ in m/s), the peak smoldering temperature, T_{max} [°C], increases almost linearly with the concurrent wind speed, U_w [m/s], as

$$T_{max} = 53U_w + 600\text{°C} \tag{5}$$

where R^2 coefficients for both linear fits are 0.95. This trend is also similar to the smoldering combustion

of coal under forced airflow, where the peak temperature increased from 448 ℃ to 854 ℃ as the internal airflow velocity ($U_{w,in}$) increased from 1.2 mm/s to 2.5 mm/s [38].

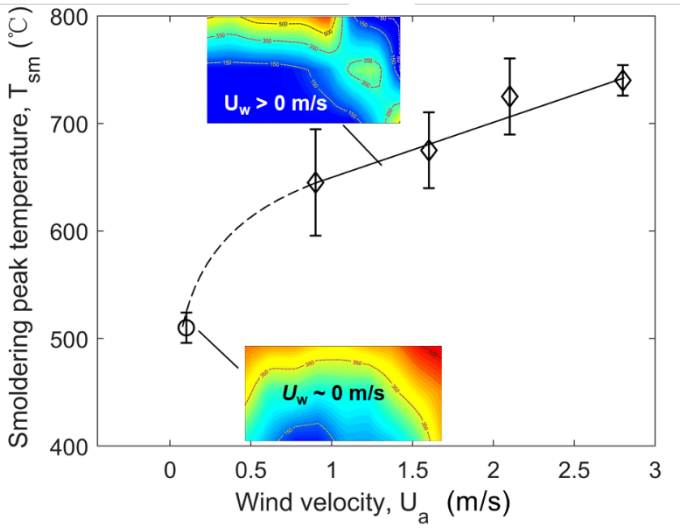

Fig. 8. Measurement of mean smoldering peak temperature as a function of wind velocity, where the error bars show the standard deviations.

3.6. Unstable smoldering-to-flaming transition

The smoldering-to-flaming (StF) transition is widely observed in charring materials such as PU foam, coal, wood, and many other biomasses [14, 16]. The StF is a quick initiation of homogeneous gas-phase flame ignition preceded by smoldering combustion, so that it is considered as an extreme fire event because of the consequent sudden increase in spread rate, power, and hazard of fire [41]. In the experiment, with large concurrent wind velocity, the StF transition was occasionally observed, as shown in Fig. 9. Initially, hot glowing spots can be observed, which may be hot enough (>1000 K) to pilot a flame, like the StF transition in other fuels [14, 42].

Fig. 9. Un-sustained smoldering-to-flaming transition under the wind velocity of 2.8 m/s.

Nevertheless, in this experiment, the flame did not spread over the entire cotton bale surface but can only sustain above the charring surface for a few minutes, and then extinguished. A similar phenomenon was also observed in the small uncompressed cotton sample in [7]. Although the oxygen supply and heat loss are two key factors that tend to govern the StF transition [18, 41], the critical condition for the flame to sustain is still unclear, but could be related to the pyrolysis chemistry and the physical properties (e.g. density, porosity and permeability). In general, the flame tends to sustain in fuel with a high volatile content, which releases more gases fuel, and a fuel with a low density, high porosity, and high permeability, which facilitate the oxygen transport, because the oxygen consumption rate of the flame is much higher than that of smoldering [43]. The sustainability of flame after the occurrence of StF and the effect of steel wire rope require further investigation and verification.

4. Conclusions

In this work, we investigated the smoldering spread of densely packed cotton bale (36 L and 225 kg/m^3) under the concurrent wind up to 2.8 m/s. We found that the smoldering spread of cotton bale is very sensitive to the wind velocity. Under a near-zero wind, the smoldering spread was extremely slow (about 10 cm/h) and showed two stages, (I) surface spread until the smoldering front covered the entire surface, and then (II) the in-depth spread from the surface to internal. With a concurrent wind, surface spread and internal spread took place simultaneously. Although the spread rate near the free surface was clearly faster, only one major concurrent-spread front was formed and spread forwards. Also, the steel wire rope can effectively slow down the surface smoldering spread by about 10 cm/h.

As the wind velocity increased, both smoldering spread rates on the free surface and inside the cotton increase, but the internal smoldering spread is less affected by the external wind. The peak smoldering temperature increased from 510 ℃ to 750 ℃, as the wind velocity increases from near zero to 2.8 m/s. Moreover, the smoldering-to-flaming transition was occasionally observed, but the flame could not be sustained. This research improves our understanding of wind effect and different spread modes for the fire of compressed porous fuel and helps evaluate the fire risk of cotton fire during transportation and storage.

Acknowledgment

This work was supported by the National Key R&D Program of China (2017YFC0805900), National Natural Science Foundation of China (NSFC) No. 51876183, the Fundamental Research Funds for the Central Universities (WK2320000041, WK2320000043), and the SKLFS Open Fund (No. HZ2019-KF02).

References

1. Wakelyn PJ, Bertoniere NR, French AD, et al (2007) Cotton Fiber Chemistry and Technology, Third. Taylor & Francis Group, Boca Raton
2. (2013) Natural fibres: Cotton. In: Wayback Mach.
3. Zhou Y, Liu W, Ni Z, et al (2017) Effects of Different Packing Materials on Cotton Fires. IOP Conf Ser Earth Environ Sci 100:. https://doi.org/10.1088/1755-1315/100/1/012085
4. Zhao X, Xiao H, Wang Q, et al (2013) Study on spontaneous combustion risk of cotton using a micro-calorimeter technique. Ind Crops Prod 50:383–390. https://doi.org/10.1016/j.indcrop.2013.07.064
5. Hagen BC, Frette V, Kleppe G, Arntzen BJ (2013) Effects of heat flux scenarios on smoldering in cotton. Fire Saf J 61:144–159. https://doi.org/10.1016/j.firesaf.2013.08.001
6. Hagen BC, Frette V, Kleppe G, Arntzen BJ (2011) Onset of smoldering in cotton: Effects of density. Fire Saf J 46:73–80. https://doi.org/10.1016/j.firesaf.2010.09.001
7. Hagen BC, Frette V, Kleppe G, Arntzen BJ (2015) Transition from smoldering to flaming fire in short cotton samples with asymmetrical boundary conditions. Fire Saf J 71:69–78. https://doi.org/10.1016/j.firesaf.2014.11.004
8. Hagen BC (2013) Onset of smoldering and transition to flaming fire. University of Bergen
9. Wakelyn PJ, Hughs SE (2002) Evaluation of the flammability of cotton bales. Fire Mater 26:183–189. https://doi.org/10.1002/fam.795
10. Gaan S, Sun G (2007) Effect of phosphorus flame retardants on thermo-oxidative decomposition of cotton. Polym Degrad Stab 92:968–974. https://doi.org/10.1016/j.polymdegradstab.2007.03.009
11. Luo Q, Ren T, Liang D, et al (2017) A study on the thermal decomposition temperature (TDT) and critical ambient temperature (CAT) of cotton. J Therm Anal Calorim 128:1617–1625. https://doi.org/10.1007/s10973-017-6090-1
12. Huang X, Gao J (2020) A Review of Near-Limit Fire Spread in Opposed Flow. Fire Saf J [invited Rev

13. Huang X, Rein G (2016) Thermochemical conversion of biomass in smouldering combustion across scales: The roles of heterogeneous kinetics, oxygen and transport phenomena. Bioresour Technol 207:409–421. https://doi.org/10.1016/j.biortech.2016.01.027
14. Boonmee N, Quintiere JG (2002) Glowing and flaming autoignition of wood. Proc Combust Inst 29:289–296. https://doi.org/10.1016/S1540-7489(02)80039-6
15. Lin S, Huang X, Urban J, et al (2019) Piloted ignition of cylindrical wildland fuels under irradiation. Front Mech Eng 5:54. https://doi.org/10.3389/fmech.2019.00054
16. Lin S, Sun P, Huang X (2019) Can peat soil support a flaming wildfire? Int J Wildl Fire 28:601–613. https://doi.org/10.1071/wf19018
17. Stoliarov SI, Zeller O, Morgan AB, Levchik S (2018) An experimental setup for observation of smoldering-to-flaming transition on flexible foam/fabric assemblies. Fire Mater 42:128–133. https://doi.org/10.1002/fam.2464
18. Rein G (2014) Smoldering Combustion. SFPE Handb Fire Prot Eng 2014:581–603. https://doi.org/10.1007/978-1-4939-2565-0_19
19. Wang S, Huang X, Chen H, Liu N (2017) Interaction between flaming and smouldering in hot-particle ignition of forest fuels and effects of moisture and wind. Int J Wildl Fire 26:71–81. https://doi.org/10.1071/WF16096
20. Putzeys O, Bar-Ilan A, Rein G, et al (2007) The role of secondary char oxidation in the transition from smoldering to flaming. Proc Combust Inst 31:2669–2676. https://doi.org/10.1016/j.proci.2006.08.006
21. Ohlemiller TJ (1985) Modeling of smoldering combustion propagation. Prog Energy Combust Sci 11:277–310. https://doi.org/10.1016/0360-1285(85)90004-8
22. Bilbao R, Mastral JF, Aldea ME, et al (2001) Experimental and theoretical study of the ignition and smoldering of wood including convective effects. Combust Flame 126:1363–1372. https://doi.org/10.1016/S0010-2180(01)00251-6
23. Huang X, Restuccia F, Gramola M, Rein G (2016) Experimental study of the formation and collapse of an overhang in the lateral spread of smouldering peat fires. Combust Flame 168:393–402. https://doi.org/10.1016/j.combustflame.2016.01.017
24. Torero JL, Fernandez-Pello a. C, Kitano M (1993) Opposed Forced Flow Smoldering of Polyurethane Foam. Combust Sci Technol 91:95–117. https://doi.org/10.1080/00102209308907635
25. Torero JL, Fernandez-Pello AC (1996) Forward smolder of polyurethane foam in a forced air flow. Combust Flame 106:89–109. https://doi.org/10.1016/0010-2180(95)00245-6
26. Torero JL, Fernandez-Pello AC (1995) Natural convection smolder of polyurethane foam, upward propagation. Fire Saf J 24:35–52. https://doi.org/10.1016/0379-7112(94)00030-J
27. Wang JH, Chao CYH, Kong W (2003) Experimental study and asymptotic analysis of horizontally forced forward smoldering combustion. Combust Flame 135:405–419. https://doi.org/10.1016/j.combustflame.2003.07.001
28. Palmer KN (1957) Smouldering combustion in dusts and fibrous materials. Combust Flame 1:129–154. https://doi.org/10.1016/0010-2180(57)90041-X
29. Lin S, Huang X (2020) Quenching of Smoldering: Effect of Wall Cooling on Extinction [under review]. Proc Combust Inst
30. Huang X, Rein G (2019) Upward-and-downward spread of smoldering peat fire. Proc Combust Inst 37:4025–4033. https://doi.org/10.1016/j.proci.2018.05.125
31. Wang ZS, Liu WF, Ni ZP, et al (2018) An Experimental Investigation on the Effect of Wind Speed on Cotton Combustion. Procedia Eng 211:788–793. https://doi.org/10.1016/j.proeng.2017.12.076
32. Wu D, Schmidt M, Huang X, Verplaetsen F (2017) Self-ignition and smoldering characteristics of coal dust accumulations in O2/N2 and O2/CO2 atmospheres. Proc Combust Inst 36:3195–3202. https://doi.org/10.1016/j.proci.2016.08.024
33. Wu D, Huang X, Norman F, et al (2015) Experimental investigation on the self-ignition behaviour of coal dust accumulations in oxy-fuel combustion system. Fuel 160:245–254. https://doi.org/10.1016/j.fuel.2015.07.050
34. Zik O, Moses E (1998) Fingering instability in solid fuel combustion: The characteristic scales of the developed state. Symp Combust 27:2815–2820. https://doi.org/10.1016/S0082-

0784(98)80139-2
35. Olson SL, Baum HR, Kashiwagi T (1998) Finger-like smoldering over thin cellulosic sheets in microgravity. Symp Combust 27:2525–2533. https://doi.org/https://doi.org/10.1016/S0082-0784(98)80104-5
36. Incropera FP (2007) Fundamentals of heat and mass transfer. John Wiley
37. Loh H-TT, Fernandez-Pello AC, Fernandez-pello CA, et al (1984) A study of the controlling mechanisms of flow assisted flame spread. Twent Symp Combust 20:1575–1582. https://doi.org/http://dx.doi.org/10.1016/S0082-0784(85)80652-4
38. Qi G, Wang D, Zheng K, et al (2016) Smoldering combustion of coal under forced air flow: Experimental investigation. J Fire Sci 34:267–288. https://doi.org/10.1177/0734904116643331
39. J.Ohlemiller T (1990) moldering combustion propagation through a permeable horizontal fuel layer. Combust Flame 81:341–353. https://doi.org/https://doi.org/10.1016/0010-2180(90)90030-U
40. Rebaque V, Ertesvåg IS, Mikalsen RF, Steen-Hansen A (2020) Experimental study of smouldering in wood pellets with and without air draft. Fuel 264:116806. https://doi.org/10.1016/j.fuel.2019.116806
41. Santoso MA, Christensen EG, Yang J, Rein G (2019) Review of the Transition From Smouldering to Flaming Combustion in Wildfires. 5:. https://doi.org/10.3389/fmech.2019.00049
42. Hu Y, Christensen EG, Amin HMF, et al (2019) Experimental study of moisture content effects on the transient gas and particle emissions from peat fires. Combust Flame 209:408–417. https://doi.org/10.1016/j.combustflame.2019.07.046
43. Quintiere JG (2006) Fundamental of Fire Phenomena. John Wiley, New York

Appendix

The thermal analysis (both TGA and DSC) was conducted with a PerkinElmer STA 6000 Simultaneous Thermal Analyzer. Before analysis, the cotton sample was first pulverized and then dried at 105 ℃ for 20 min. The initial mass of cotton was about 5 mg, and sample was heated at a constant rate of 10 K/min. Test environments with two oxygen concentrations were selected, 0% (nitrogen) and 21% (air), with a flow rate of 50 mL/min. **Figure A1** shows the mass-loss rate and heat flow curves of this cotton sample. As indicated by the fast increase of mass loss rate and heat release rate, the thermal and oxidative decomposition of cotton starts at about 250 ℃. The heat of smoldering combustion can be calculated by integrating the heat flow curve in Fig. A1(b), and for this cotton sample, the calculated value is ~ 10 MJ/kg which is smaller than 16 MJ/kg for the heat of flaming combustion [10].

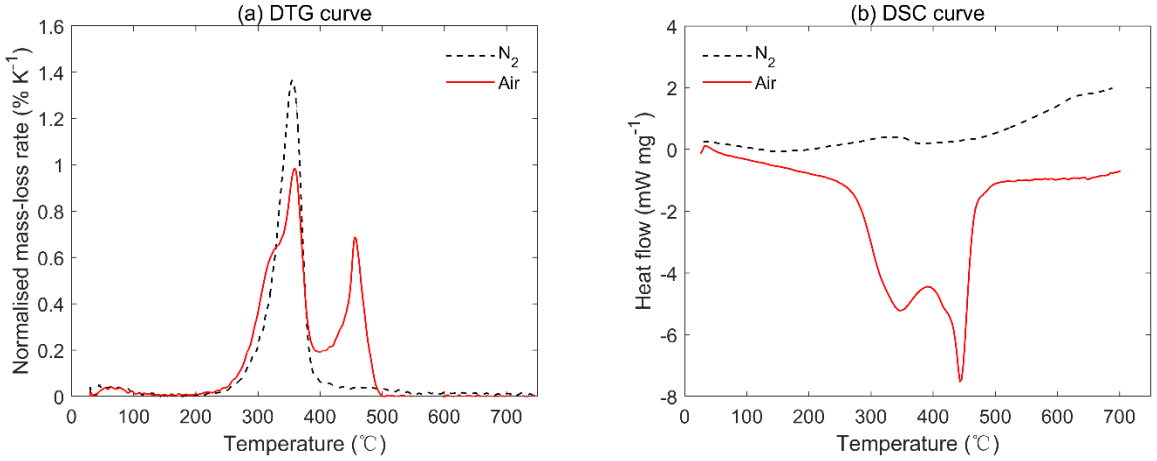

Fig. A1. TGA-DSC curves of cotton sample under air and nitrogen flow at a heating rate of 10 K/min, (a) normalized mass loss rate; and (b) heat flow as a function of temperature where is the differentiated TG or the mass loss rate.

Link for download videos:

Video 1: Top-view video for smoldering spread over cotton without wind, where video play speed is 100 times normal speed. https://youtu.be/dLAMLEdC1_A

Video 2: Top-view video for smoldering spread over cotton with concurrent wind speed of 2.8 m/s, where video play speed is 100 times normal speed. https://youtu.be/gT1Ubvw7VWA

Video 3: Front-view thermal imaging inside cotton based on thermocouple matrix measurement without wind, where video play speed is 100 times normal speed. https://youtu.be/fybTHeiwqjQ

Video 4: Front-view thermal imaging inside cotton based on thermocouple matrix measurement with concurrent wind speed of 2.8 m/s, where video play speed is 100 times normal speed. https://youtu.be/vdU6Y7b5Rnk

For inquiries, please contact Qiyuan Xie xqy@ustc.edu.cn and Xinyan Huang xy.huang@polyu.edu.hk